Korean J. Chem. Eng., 33(1), 255-259 (2016)
DOI: 10.1007/s11814-015-0125-8

pISSN: 0256-1115
eISSN: 1975-7220

Hydrogen bond dynamics in liquid water: Ab initio molecular dynamics simulation

Cheolhee Kim*, Min Sun Yeom,†, and Eunae Kim*,†**

*College of Pharmacy, Chosun University, Gwangju 501-759, Korea
**Korea Institute of Science and Technology Information, 245, Daehang-ro, Yoseong-gu, Daejeon 305-806, Korea
(*Received 17 March 2015 • accepted 12 June 2015*)

Abstract−The effect of intermolecular interaction on the distribution of the harmonic vibrational frequencies of water molecules was investigated through ab initio molecular dynamics simulations based on the Born-Oppenheimer approach. For single water, the effect of the dynamics of the oxygen atom in single water and the simulation time step on the frequency distribution were examined. The distributions of the OH stretching and HOH bending vibrational frequencies of liquid water were compared to those of single water. The probability distributions of the change in OH bond length and the lifetime of the dangling OH bond were also obtained. The distribution of the frequencies was strongly affected by the long lifetime of the dangling OH bond, resulting in the formation of hydrogen bonds between water molecules.

Keywords: Ab Initio Molecular Dynamics Simulation, Born-oppenheimer Approach, Water, Hydrogen Bond, Vibrational Frequency

INTRODUCTION

The water detected in interstellar clouds is one of the most abundant molecules in the universe. Water is also vital for all life on earth and plays crucial roles in many metabolic processes, photosynthesis, and enzyme function. Recently, the structure and function of internal water molecules in biopolymers have been studied [1-7] For example, by means of low-temperature Fourier-transform infrared (FTIR) spectroscopy, Hashimoto et al. [1] found that Gloeobacter rhodopsin (GR) possesses strongly hydrogen-bonded water molecules. They observed that there is a strong correlation between the proton-pumping activity and strongly hydrogen-bonded water molecules. Water vapor, the tiny water droplets in clouds and ice clouds absorb solar radiation so that the water causes a greenhouse effect [8-16]. In particular, water clusters (clusters of water molecules including water dimmers) act as greenhouse gases. Many studies on water clusters have been carried out not only to investigate the role of water clusters in biological and chemical systems and but also to understand the nature of hydrogen bonding [8-11,13-28]. The geometries and harmonic vibrational frequencies of water monomers and clusters have also been studied [11,13-17,19,20,25]. The OH-stretching and HOH-bending vibrational band positions and intensities have been reported for water clusters. Frequency peaks corresponding to hydrogen-bonded and free OH bonds have been observed [13,15,25]. Kandori and Shichida [12] studied the stretching vibrations of a bridged water molecule inside a protein in bacteriorhodopsin to investigate the role of bridged water in active proton transport. They observed widely distributed O-D stretching vibrational frequencies for the bridged water. A high-frequency OH stretching peak arising from the hydration shell around nonpolar solute groups was observed by using a combination of vibrational spectroscopy and multivariate curve resolution [24]. Kumar et al. [21] also studied the relation between hydrogen bonding and the vibrational frequency spectra of water on the surface of rutile. They found strong adsorption sites produced by strong hydrogen bonds formed between the surface oxygen atoms and the absorbed water molecules. In liquid water, many vibrational frequency peaks have been observed experimentally [22,23,27,28] and theoretically [18,26], and assigned to intermolecular stretchings and bendings, librations, intramolecular symmetric and asymmetric stretchings, and intramolecular bendings. Hydrogen bonding in liquid water induces a lower frequency for the main stretching band and a higher bending frequency. In this work, we obtained the distribution of the harmonic vibrational frequencies of liquid water through ab initio molecular dynamics simulations. We compared the calculated intermolecular harmonic vibrational frequencies of liquid water with the data obtained previously, and discuss the frequency distributions. We investigated the lifetimes of hydrogen-bonded structures in liquid water. The effects of hydrogen bonds on the dynamics of the water molecules and on the distribution of the harmonic vibrational frequencies are also discussed.

COMPUTATIONAL DETAILS

Ab initio molecular dynamics simulations based on the Born-Oppenheimer approach were performed for single water and liquid water systems at 298.15 K. All calculations were performed using Quickstep [29] based on the Gaussian and plane wave (GPW) method and its augmented extension, the Gaussian and augmented plane-wave (GAPW) method. In this work, the GAPW method

†To whom correspondence should be addressed.
E-mail: eunaekim@chosun.ac.kr, msyeom@kisti.re.kr
‡This article is dedicated to Prof. Hwayong Kim on the occasion of his retirement from Seoul National University.

using DZVP basis sets and an energy cutoff of 300 Rydberg (Ry) were used. 32 water molecules were used in a cubic box of length 9.8528 Å for the density of liquid water systems (ρ=1.0 kg/L). The PBE exchange-correlation energy functional and the orbital transformation were employed. Periodic boundary conditions were applied in all directions, and time steps of 0.1, 0.5, and 1.0 fs were used to investigate the lifetimes of hydrogen bonded structures in liquid water. For the calculation of the harmonic vibrational frequencies of water molecules, the dynamics of single water and of water molecules was analyzed over 200,000 time steps.

RESULTS AND DISCUSSION

1. Harmonic Vibrational Frequencies

Kim et al. [20] calculated the harmonic vibrational frequencies of a water monomer. They obtained the symmetric stretching, asymmetric stretching and bending frequencies by through various levels of ab initio molecular dynamics simulations using various basis sets and compared the calculated frequencies with the experimental data [17] of 3,832.2 cm^{-1}, 3,942.5 cm^{-1}, and 1,648.5 cm^{-1}, respectively. They reported that the root mean square deviations of these three vibrational frequencies ranged from 1 to 255 cm^{-1}. In this work, ab initio molecular dynamics simulations were performed for single water and liquid water systems at three different time steps. The distributions of the stretching vibrational frequencies are shown in Fig. 1. The average values at the time steps of 0.1, 0.5, and 1.0 fs are 3,689, 3,709, and 3,774 cm^{-1}, respectively. The range of frequencies increased as the simulation time step increased. The maximum probability also increased with the time step. The lower average frequency, narrower range of frequencies, and lower maximum probability at smaller time steps are considered to be due to the degree of precision. We also calculated the distribution when the position of the oxygen atom was fixed, in order to understand the effect of the dynamics of the oxygen atom on the harmonic vibrational frequencies of the water monomer. The average values at the time steps of 0.1, 0.5, and 1.0 fs are 3,590, 3,685, and 3,751 cm^{-1},

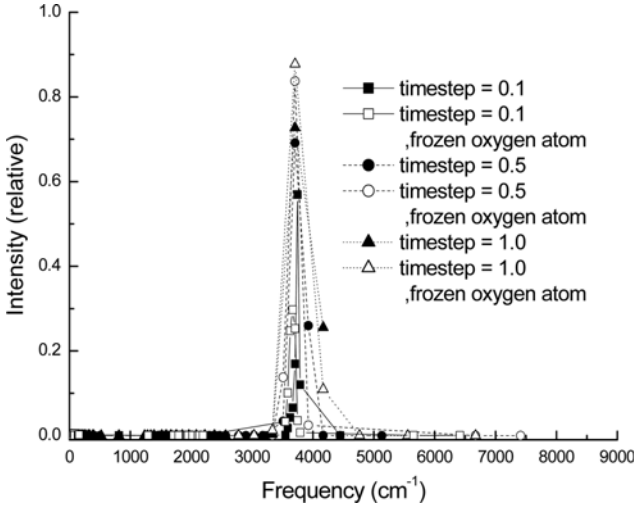

Fig. 1. Distribution of OH stretching vibrational frequencies of a water monomer.

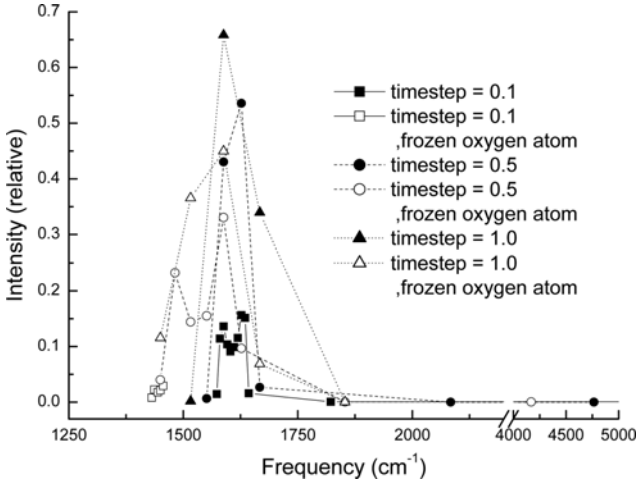

Fig. 2. Distribution of HOH bending vibrational frequencies of the water monomer.

respectively. When the oxygen atom is frozen, the averages decrease and the maximum probabilities increase. The restricted dynamic behavior of the oxygen atom of a water monomer causes sparsely distributed frequencies. Therefore, the dynamics of the oxygen atom induces lightly higher stretching vibrational frequencies.

The bending vibrational frequencies were also calculated from the trajectories obtained from ab initio molecular dynamics simulations. The distribution of the HOH bending vibrational frequencies of the water monomer is shown in Fig. 2. The calculated average bending vibrational frequencies at the time steps of 0.1, 0.5, and 1.0 fs are 1,616, 1,611, and 1,615 cm^{-1}, respectively. The computed average bending vibrational frequencies of the water monomer are very similar regardless of the time step, and are also similar to the experimental data. However, unlike the stretching frequency distribution, there are no low bending frequencies. The average HOH bending vibrational frequencies of the water monomer with a frozen oxygen atom decrease relative to those with free oxygen. The average values at time steps of 0.1, 0.5, and 1.0 fs are 1,531, 1,547, and 1,551 cm^{-1}, respectively. Even though the average values are very similar regardless of the time step, the distributions are different at each time step. The frequencies with short time steps (0.1 and 0.5 fs) are mostly distributed between 1,430 and 1,853 cm^{-1}, except for one very high frequency of around 5,000 cm^{-1}. The distribution does not have a steep peak. At the time step of 1.0 fs, all the frequencies are distributed between 1,450 and 1,853 cm^{-1}, and the distribution peak is very steep. Therefore, the dynamics of the oxygen atom have a stronger influence on the bending frequencies than on the stretching frequencies.

The dynamics and structure of small-sized water clusters are very important for understanding their role in human life, including in active proton and the absorption of solar radiation. Furthermore, this information provides a key to understanding the dynamics and structure of liquid water. Many experimental and theoretical studies on OH stretching and HOH bending vibrations in water clusters have been carried out [11,13,15,20,25]. The authors have reported several absorption bands of small water clusters located from 3,300 to 3,800 cm^{-1} for the bonded OH stretching and free

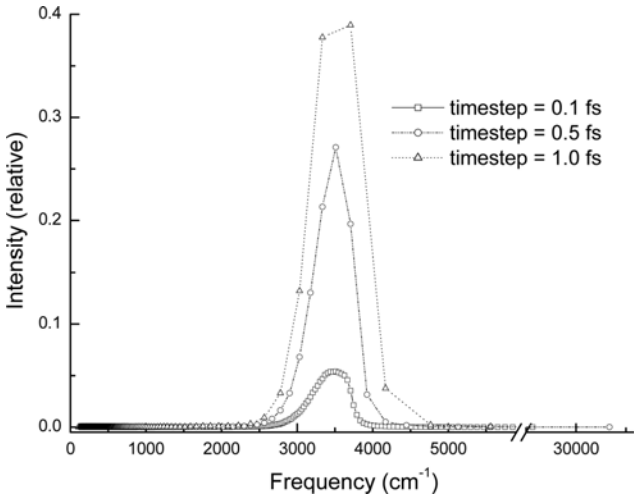

Fig. 3. Distribution of OH stretching vibrational frequencies of liquid water.

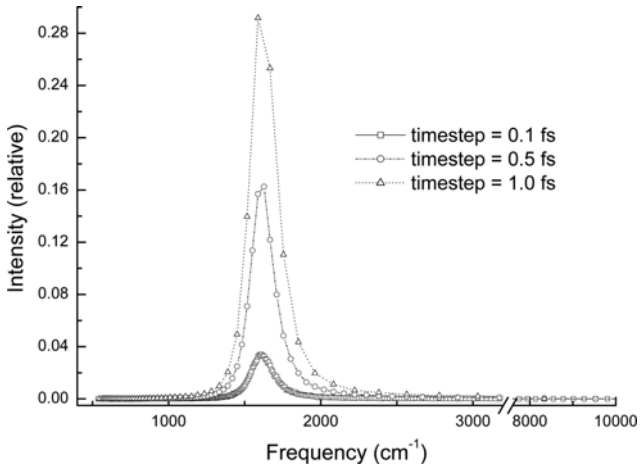

Fig. 4. Distribution of HOH bending vibrational frequencies of liquid water.

OH stretching vibrations, and from 1,600 to 1,640 cm^{-1} for the HOH bending vibrations. For liquid water, previous studies obtained absorption bands located at around 3,400, 1,650, 650 and 170 cm^{-1}, which can be assigned to the stretching, bending, libration, and hydrogen-bonding anti-symmetric stretching vibrations, respectively [18,22,26,28]. The distribution of the harmonic vibrational frequencies of liquid water was obtained in Fig. 3. On comparison of the distribution of the stretching vibrational frequencies of liquid water with the frequencies of a water monomer, broad stretching frequencies appear in the range of 106 cm^{-1} to 33,356 cm^{-1}. The largest frequencies obtained at time steps of 0.1, 0.5, and 1.0 fs are 25,658, 33,356, and 16,678 cm^{-1}, and the highest peaks at these time steps of 0.1, 0.5, and 1.0 fs are obtained at 3,511, 3,511, and 3,335 cm^{-1}, respectively. Therefore, the highest stretching frequency peaks are obtained at the almost same frequency by varying their relative intensities. The relative intensity of the hydrogen bonded OH stretching vibration varies significantly with the time step. The average values are 3,353, 3,377, and 3,420 cm^{-1}, respectively, which are lower than those for a water monomer. It is well known that hydrogen bonding leads to changes in the OH stretching vibration. Therefore, good agreement between predicted and experimentally observed frequency shifts is established.

The effect of the hydrogen-bonding and intermolecular repulsive interactions on the bending vibration is very interesting. In general, it is believed that the bending vibrational frequencies of liquid water are found at a position slightly shifted from that of the water monomer (about 1,650 cm^{-1}). A broad distribution of bending vibrational frequencies was also obtained for liquid water, as shown in Fig. 4. The distribution was obtained at time steps of 0.1, 0.5, and 1.0 fs, at which the smallest values of the bending vibrational frequencies are 538, 551, and 546 cm^{-1}, respectively, and the largest values are 25,658, 22,237, and 16,678 cm^{-1}, respectively. The averages (1,655, 1,646, and 1,649 cm^{-1}, respectively) are larger than those of the water monomer. The shifting is in good agreement with the increase in the average HOH bending vibrational frequency in liquid water due to hydrogen bond formation. The highest bending frequency peaks are also obtained at the almost same frequency by varying their relative intensities. The relative intensity of the hydrogen bonded OH bending vibration varies significantly with the time step.

2. Hydrogen Bond

For the investigation of the effect of the hydrogen bonding interaction in liquid water on the harmonic vibrational frequencies, the probability distribution of the change in bond length ($\Delta L = L_{t+1} - L_t$) was calculated. Here, L_{t+1}, and L_t are the bond lengths at t+1 and t, respectively. The change in bond length is defined as the difference between the bond lengths calculated at two consecutive simulation steps. Therefore, a small ΔL value means a slow stretching vibration, which has a low frequency. The probability distributions of the change in bond length of liquid water and single water monomer are compared in Fig. 5, where the small ΔL value is higher for single water. The small ΔL value in single water (smaller than 0.001) might be related mainly to the change in direction of the hydrogen atoms. In liquid water, the small ΔL value (smaller than 0.001) might be related mainly to the change in direction of the hydrogen atoms and intermolecular interaction. Therefore, the difference between the smallest ΔL value of single water and that of liquid

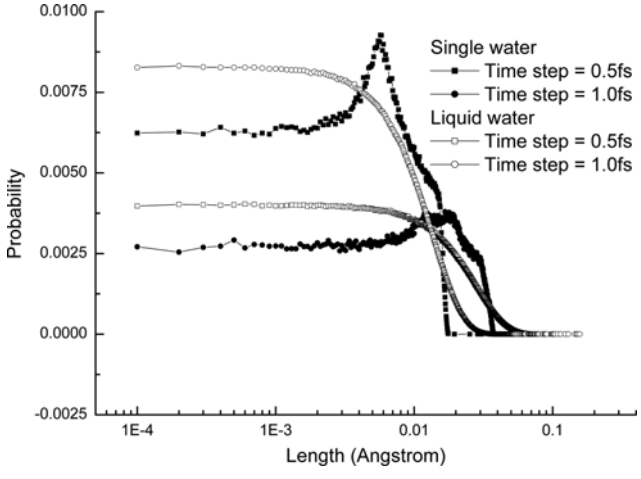

Fig. 5. Probability distribution of bond length change of liquid water.

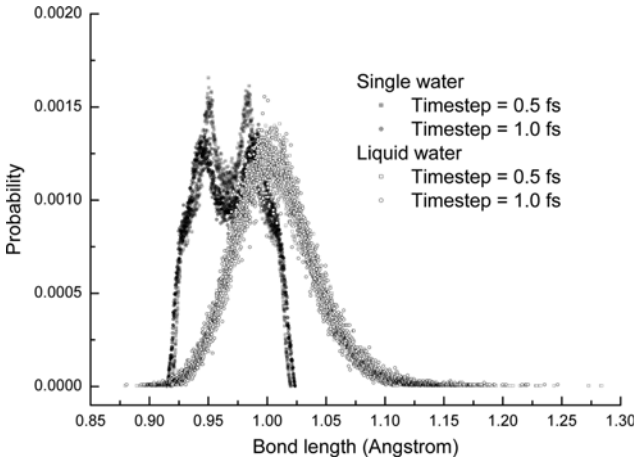

Fig. 6. Probability distribution of bond length at ΔL≤0.0002.

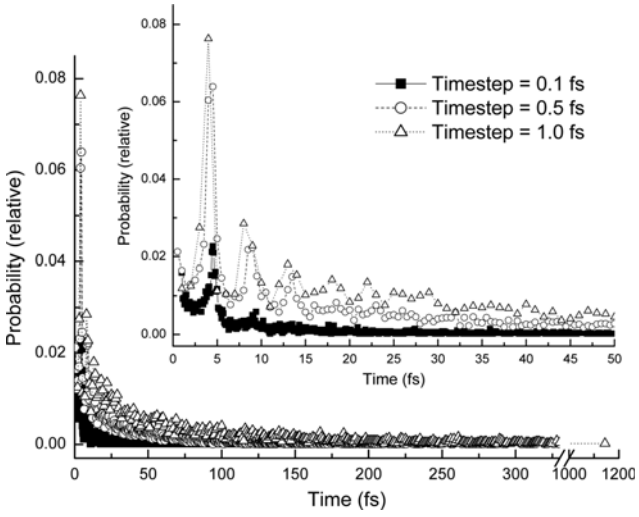

Fig. 7. Probability distribution of dangling OH bond lifetime.

water can be considered to arise because of the change in lifetime of the dangling OH-bond due to hydrogen bonding. In liquid water, a large ΔL value, which must be due to intermolecular repulsive interactions, is observed. As the time step increases, the small ΔL value decreases, whereas the large ΔL increases. The effect of the dynamics of the oxygen atom on the probability distribution of the change in bond length was also studied. The probability distribution was obtained by using an energy cutoff of 600 Rydberg (Ry) and a convergence tolerance ten times smaller than this cutoff. The distribution is not affected by the energy cut-off and the convergence tolerance.

In Fig. 6, the probability distributions of the bond length at ΔL≤ 0.0002 and time steps of 0.5 and 1.0 fs are shown. A low probability at around the average bond length at ΔL≤0.0002 (0.969 Å) of the water monomer was found, which arises because the small ΔL is due to the change in direction of the hydrogen atoms. However, for liquid water, there is a Gaussian-like distribution centered at the average bond length at ΔL≤0.0002 (1.007 Å). This is clear evidence that hydrogen bonding interactions generate low stretching vibrational frequencies.

The average changes in bond length (ΔL_{ave}) at two consecutive simulation steps were calculated to be 1.5×10^{-3} Å, 7.7×10^{-3} Å, and 1.6×10^{-2} Å at time steps of 0.1, 0.5, and 1.0 fs, respectively. Here, we define a dangling OH-bond as one when the change in bond length is smaller than $0.2\times\Delta L_{ave}$. The probability distribution of the bond lifetime satisfying the dangling OH-bond condition was calculated. For single water, the maximum lifetimes at time steps of 0.1, 0.5 and 1.0 fs are less than 1.0 fs because of the maximum time step of 1.0 fs. If there are short lifetimes satisfying the dangling OH-bond condition, these come from change in direction of the hydrogen atoms arising because of the lack of intermolecular interaction. However, for liquid water, a long lifetime was obtained. Fig. 7 shows the probability distribution of the lifetime of the dangling OH-bond in liquid water. The maximum peaks are obtained at 4.5, 4.5, and 4.0 fs for time steps of 0.1, 0.5, and 1.0 fs, respectively. Even though the maximum intensities are obtained at similar lifetimes, the average values increase as the time step increases. The average values and maximum lifetimes are related to the different criteria. $0.2\times\Delta L_{ave}$, which is used as a criterion, is 3.0×10^{-4} Å, 1.54×10^{-3} Å, and 3.2×10^{-3} Å at time steps of 0.1, 0.5, and 1.0 fs, respectively. The maximum lifetimes are 510, 488, and 1,144 fs at time steps of 0.1, 0.5, and 1.0 fs, respectively. If a dangling OH-bond is defined as one for which the change in bond length is smaller than $0.2\times\Delta L_{ave}$ ($=1.5\times10^{-3}$) at the time step of 0.5 fs, the maximum lifetimes are 30.24 ps, 488 fs, and 179 fs at time steps of 0.1, 0.5, and 1.0 fs, respectively.

CONCLUSIONS

We performed ab initio molecular dynamics simulations to investigate the effect of intermolecular interactions on the distribution of the harmonic vibrational frequencies of water molecules. The frequency distributions for single water and liquid water were obtained at three different time steps. The range of frequencies increased as the simulation time step was increased. The maximum probability also increased with the time step. The lower average frequency, narrower range of frequencies, and the maximum probability at smaller time steps were considered to be due to the degree of precision. We also calculated the distribution when the position of the oxygen atom was fixed, in order to understand the effect of the dynamics of the oxygen atom on the harmonic vibrational frequencies of the water monomer. The restricted dynamic behavior of the oxygen atom of a water monomer gave rise to sparsely distributed frequencies. Therefore, the dynamics of the oxygen atom induce slightly higher stretching vibrational frequencies. The computed average bending vibrational frequencies of the water monomer were very similar regardless of the time step. The average HOH bending vibrational frequencies of the water monomer with a frozen oxygen atom were lower than those with free oxygen. Therefore, the dynamics of the oxygen atom has a stronger influence on the bending frequencies than on the stretching frequencies. The distribution of the harmonic vibrational frequencies of liquid water was obtained. A broader stretching frequency distribution was obtained for liquid water than that for the water monomer. This is because of the effect of the hydrogen-bonding and intermolecular repulsive interactions. The probability distributions for the change

in OH bond length and the lifetime of the dangling OH bond were also obtained. For liquid water, we obtained a Gaussian-like distribution for the change in OH bond length, which is clear evidence of hydrogen-bonding interactions. The hydrogen-bonding interaction also induces a long lifetime of the dangling OH bond. Therefore, the frequency distribution is strongly affected by the hydrogen-bonding interaction.

ACKNOWLEDGEMENT

This study was supported by research fund from Chosun University, 2012. Also we thank KISTI supercomputing center for providing supercomputing resources (KSC-2013-C3-063).

REFERENCES

1. K. Hashimoto, A. R. Choi, Y. Furutani, K. H. Jung and H. Kandori, *Biochem.*, **49**, 3343 (2010).
2. U. Haupts, J. Tittor and D. Oesterhelt, *Annu. Rev. Biophys. Biomol. Struct.*, **28**, 367 (1999).
3. H. Kandori, Y. Yamazaki, J. Sasaki, R. Needleman, J. K. Lanyi and A. Maeda, *J. Am. Chem. Soc.*, **117**, 2118 (1995).
4. H. Kandori, *Biochim. Biophys. Acta*, **1460**, 177 (2000).
5. J. K. Lanyi, *J. Struct., Bio.*, **124**, 164 (1998).
6. H. Luecke, B. Schobert, H. T. Richter, J. P. Cartailler and J. K. Lanyi, *J. Mol. Biol.*, **291**, 899 (1999).
7. A. Maeda, J. Sasaki, Y. Yamazaki, R. Needleman and J. K. Lanyi, *Biochem.*, **33**, 1713 (1994).
8. J. Daniel, S. Solomon, R. Saunders, R. Portman, D. Miller and W. Madsen, *J. Geophys. Res.*, **104**, 16785 (1999).
9. J. S. Daniel, S. Solomon, H. G. Kjaergaard and D. P. Schofield, *Geophys. Res. Lett.*, **31**, L06118 (2004).
10. C. Hill and R. Jones, *J. Geophys. Res.*, **105**, 9421 (2000).
11. F. Huisken, M. Kaloudis and A. Kulcke, *J. Chem. Phys.*, **104**, 17 (1996).
12. H. Kandori and Y. Shichida, *J. Am. Chem. Soc.*, **122**, 11745 (2000).
13. G. R. Low and H. G. Kjaergaard, *J. Chem. Phys.*, **110**, 9104 (1999).
14. I. V. Ptashnik, K. M. Smith, K. P. Shine and D. A. Q. Newnham, *J. R. Meteorol. Soc.*, **130**, 2391 (2004).
15. D. P. Schofield and H. G. Kjaergaard, *Phys. Chem. Chem. Phys.*, **5**, 3100 (2003).
16. V. Vaida, J. Daniel, H. G. Kjaergaard, L. M. Goss and A. F. Q. Tuck, *Meteorol. Soc.*, **127**, 1627 (2001).
17. W. S. Benedict, N. Gailar and E. K. Plyler, *Chem. Phys. Lett.*, **24**, 1139 (1956).
18. R. Bansil, T. Berger, M. A. R. Toukan and S. H. Chen, *Chem. Phys. Lett.*, **132**, 165 (1986).
19. L. A. Curtiss and J. A. Pople, *J. Mol. Spectros.*, **55**, 1 (1975).
20. J. Kim, J. Y. Lee, S. Lee, B. J. Mhin and K. S. Kim, *J. Chem. Phys.*, **102**, 310 (1995).
21. N. Kumar, S. Neogi, P. R. C. Kent, A. V. Bandura, J. D. Kubicki, D. J. Wesolowski, D. Cole and J. O. Sofo, *J. Phys. Chem. C*, **113**, 13732 (2009).
22. R. Oder and D. A. I. Goring, *Spectr. Acta Part A: Molecular Spectroscopy*, **27**, 2285 (1971).
23. S. Palese, J. T. Buontempo, L. Schilling, W. T. Lotshaw, Y. Tanimura, S. Mukamel and R. J. D. Miller, *J. Phys. Chem.*, **98**, 12466 (1994).
24. P. N. Perera, K. R. Fega, C. Lawrence, J. Tomlinson-Phillips and D. Ben-Amotz, *P.N.A.S.*, **106**, 12230 (2009).
25. D. P. Schofield, J. R. Lane and H. G. Kjaergaqard, *J. Phys. Chem. A*, **111**, 567 (2007).
26. P. L. Silvestrelli, M. Bernasconi and M. Parrinello, *Chem. Phys. Lett.*, **277**, 478 (1997).
27. L. Thrane, R. H. Jacobsen, P. U. Jepsen and S. R. Keiding, *Chem. Phys. Lett.*, **240**, 330 (1995).
28. K. N. Woods and H. Wiedemann, *Chem. Phys. Lett.*, **393**, 159 (2004).
29. J. VandeVondele, M. Krack, F. Mohamed, M. Parrinello, T. Chassaing and J. Hutter, *Comp. Phys. Comm.*, **167**, 103 (2005).